

Novel Dual-Band Microwave Filter using Dual-Capacitively-Loaded Cavity Resonators

Xiaoguang Liu, *Student Member, IEEE*, Linda P. B. Katehi, *Fellow, IEEE*, and Dimitrios Peroulis, *Member, IEEE*

Abstract—We present a novel design concept for low-loss dual-band cavity filters based on dual-capacitively-loaded (DCL) cavity resonators. The relatively independent control over the center frequencies, inter-resonator and external coupling coefficients makes the DCL resonator an ideal building block for dual-band filters with widely separated passbands. The high unloaded quality factor (Q_u) of the DCL cavity resonator ensures a low insertion loss. An example 2-pole dual-band filter at 2.4 GHz and 5.0 GHz is demonstrated with an insertion loss of 1.47 dB at 2.4 GHz, 1.01 dB at 5.0 GHz and a bandwidth of 24.8 MHz ($\sim 1\%$) at 2.4 GHz, and 51.2 MHz ($\sim 1\%$) at 5.0 GHz.

Index Terms—dual-band filter, waveguide filter, quality factor, cavity resonator

I. INTRODUCTION

Recently, dual-band and multi-band RF/microwave filters have attracted significant research attention due to the growing need for multi-standard multi-frequency wireless communication systems [1]–[7]. Conventionally, dual-band filters are designed by parallel integration of two band-pass filters using duplexing elements [1] or cascading a band-stop filter with a band-pass filter to create multiple pass bands [2]. Direct synthesis of dual-band filters is also possible by proper frequency transformations [3], [4]. More recently, dual-band filter designs based on dual-resonance resonators have become popular as they allow for easy placement of the two passbands. These filters are predominantly based on various forms of stepped-impedance resonators (SIR) realized in microstrip form [5]–[7]. Although compact in size, such dual-band filters suffer from relatively low unloaded quality factor ($Q_u < 200$).

In this paper, we present a novel dual-band filter design methodology based on dual-capacitively-loaded (DCL) cavity resonators. Fig. 1 shows an illustration of a 2-pole filter composed of two DCL resonators. Each DCL resonator consists of a cavity and two conductive posts, both connected to the resonator on one end. The first two resonant frequencies of the DCL cavity resonator can be arbitrarily controlled, making it possible to design dual-band filters with arbitrary passband locations. The bandwidth of the two passbands can also be

This work has been supported by the Defense Advanced Research Projects Agency under the ASP Program with a subcontract from BAE Systems. The views, opinions, and/or findings contained in this article/presentation are those of the author/presenter and should not be interpreted as representing the official views or policies, either expressed or implied, of the Defense Advanced Research Projects Agency or the Department of Defense.

X. Liu and D. Peroulis are with the School of Electrical and Computer Engineering, Purdue University, West Lafayette, IN, 47906 USA e-mail: liu79@purdue.edu and dperouli@purdue.edu.

L. P. B. Katehi is with the University of California, Davis, CA, USA. email: katehi@ucdavis.edu.

Manuscript received March 03, 2010; revised June 12, 2010.

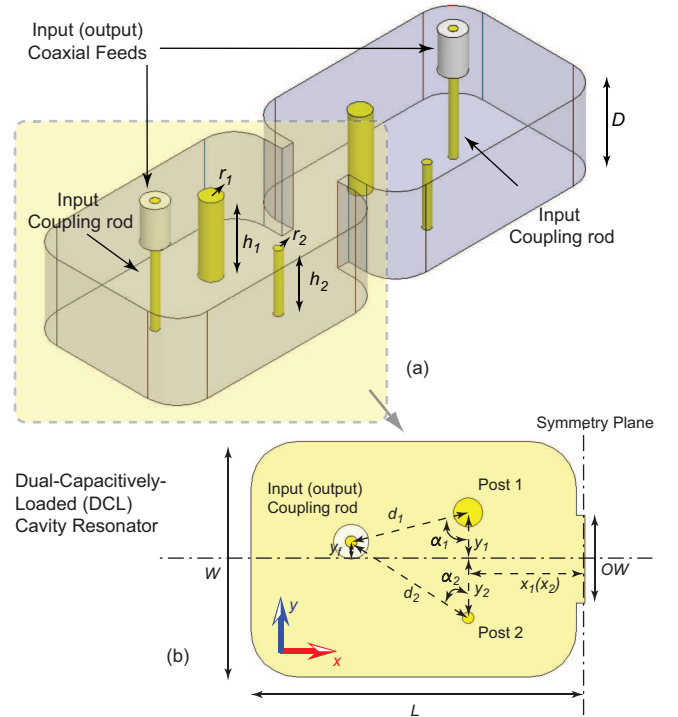


Fig. 1. (a) Illustration of a 2-pole dual-band filter using DCL resonators. (b) Top-view of the DCL resonator showing critical design dimensions.

individually adjusted. The high Q_u (> 1000) makes DCL resonators ideal building blocks for low-loss dual-band filters.

II. DUAL-CAPACITIVELY-LOADED (DCL) RESONATOR

When a cavity resonator is loaded by two conductive posts of different sizes (Fig. 1), it is observed that the first two resonant frequencies f_1 and f_2 can be adjusted individually by the size and position of the two posts. Fig. 2 shows the simulated f_1 and f_2 of a DCL cavity resonator with different capacitive post sizes. The cavity size is $1.6 \times 2.5 \times 1 \text{ in}^3$. Simulation is conducted with Ansoft HFSS [8] (eigenmode).

As shown in Fig. 2, a unique characteristic of the DCL resonators is that the tuning of one of the two lowest frequencies has a minimal effect on the other, provided that the resonator's dimensions are properly selected. For example, in Fig. 2(a), the height of post 1 is swept from 12 mm to 18 mm with radius r_1 of 1-4 mm. f_2 is observed to change from 2.2 GHz to 3.8 GHz (1.72 : 1) whereas f_1 changed from 5.0 GHz to 4.9 GHz (1.02 : 1). A similar trend can be observed in the Q_u of the DCL resonators (Fig. 2(c,d)). For example, when the height of post 1 is swept from 12 mm to 18 mm, the Q_u of the first resonance drops from 7750 to 4510, whereas the Q_u of the second resonance remains relatively unchanged ($< 5\%$).

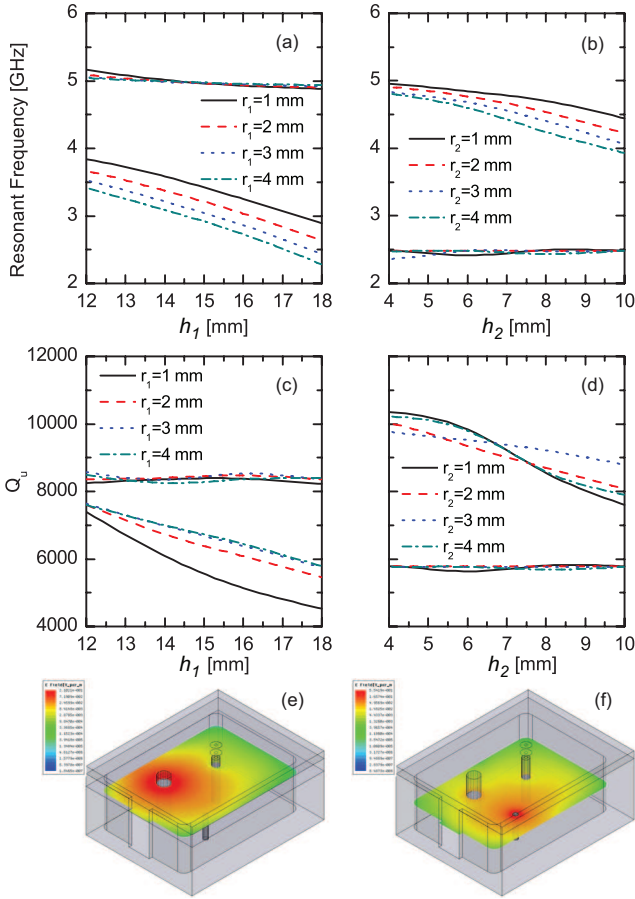


Fig. 2. (a,b) Simulated f_1 and f_2 of the DCL cavity resonator when the size of two posts are varied. (c,d) Simulated Q_v of the DCL cavity resonator when the size and height of two posts are varied. (e,f) Simulated electric field distribution inside the cavity at the first and the second resonant frequencies.

III. 2-POLE DUAL-BAND FILTER DESIGN

As shown in the previous section, the relatively independent tuning characteristic of f_1 and f_2 of a DCL cavity resonator allows the design of dual-band filters with arbitrary passband locations. By choosing the appropriate cavity dimensions and the two capacitive loading posts, the two bands can be individually chosen with a given insertion loss requirement.

For a dual-band filter design, it is desirable to be able to control the bandwidth of the two passbands individually because the two wireless standards may have different bandwidth requirements. This implies individual control of the inter-resonator coupling and external coupling of the two passbands.

The inter-resonator coupling between the two DCL cavity resonators is achieved by magnetic coupling through an open window on the resonator sidewall. The coupling coefficient (k_c) is dependent on a few parameters, such as the window width and the positions of the capacitive posts. A wider window opening generally gives higher coupling coefficients for both bands. Coupling is also stronger when the two posts are closer to the coupling window.

To achieve individual control of the inter-resonator coupling coefficients of the two passbands, the y -position (y_1 and y_2) of one pair of posts can be adjusted to tune its respective coupling without significantly affecting the coupling of the other pair.

To illustrate this, Fig. 3 shows the simulated k_{c1} and k_{c2} of the two bands when the posts' y -positions are adjusted. In Fig. 3(a), k_{c1} changes from 0.0054 to 0.003 when y_1 changes from 8 mm to 15 mm, whereas k_{c2} remains relatively unchanged ($< 5\%$). Similar behavior is observed when y_2 is adjusted for post 2 (Fig. 3).

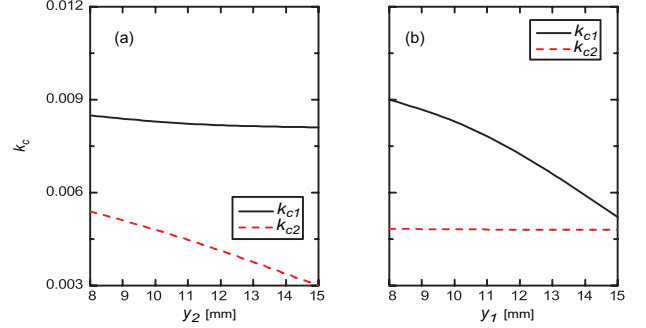


Fig. 3. Simulated inter-resonator coupling coefficients with respect to y_1 and y_2 of the posts.

The external coupling is achieved by magnetic coupling between the input (output) coupling rod and the capacitive posts (Fig. 1(a)). In general, the coupling strength is directly related to the distance (d_1 and d_2) between the coupling rod and the capacitive post and is a relatively weak function of the angular position (α_1 and α_2) of the coupling rod with respect to the capacitive post. In order to achieve individual control of the external coupling, one can follow an intuitive procedure. First, the external coupling of one band can be determined by choosing a proper distance between the coupling rod and the capacitive post. The coupling rod can then be moved along an equi-distance circle around the first post until the required external coupling to the second post is achieved. In practice, a few iterations may be needed to optimize the design.

To illustrate this, Fig. 4 shows the simulated external quality factor (Q_e) for the two bands when the post moves along the respective equi- d circles around the two posts. Q_e is calculated using the approach given in [10]. Relative independent control over the external coupling strength is observed.

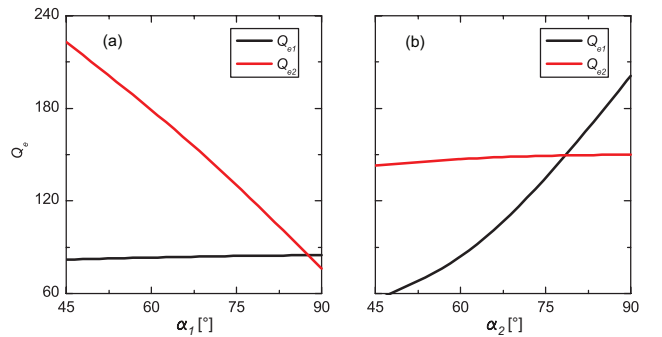


Fig. 4. Simulated Q_e with respect to α_1 and α_2 .

Fig. 5 shows the simulated S-parameters of a proof-of-concept dual-band filter at 2.4 GHz and 5.0 GHz. The overall dimension of the filter is $2 \times 5 \times 1.7$ in³. This dimension is chosen for a compromise between easy of fabrication and small volume. With capacitive posts, the filter dimension is

smaller than those of the traditional half-wavelength resonator based filters. The two post sizes are 1 mm and 2 mm in diameter and 10 mm and 18.5 mm in height respectively. The location of the input (output) coupling rod is determined by $d_1 = 21.2$ mm, $d_2 = 22.8$ mm, $\alpha_1 = 19.3^\circ$ and $\alpha_2 = 28.8^\circ$. To demonstrate the flexibility of the proposed design approach, an additional design (Design 2) for 2.8 GHz and 4.5 GHz is also included.

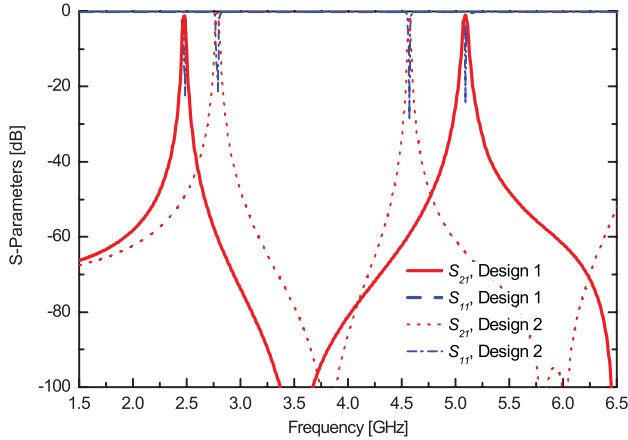


Fig. 5. Simulated S-parameters of the designed dual-band filters.

IV. MEASUREMENTS AND DISCUSSION

Fig. 6 shows the fabricated filter which is machined from copper. The four capacitive posts are machined from brass (conductivity of 1.5×10^7 S/m). Additional threaded rods are used for minor coupling adjustments to compensate for fabrication tolerances.

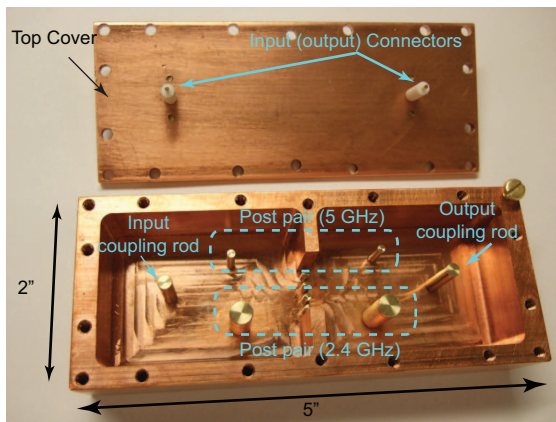


Fig. 6. Picture of the fabricated dual-band filter.

Measurement results are shown in Fig. 7. The frequency responses are in good agreement with the HFSS simulation. A measured insertion loss of 1.47 dB (0.38 dB in simulation) is achieved at 2.4 GHz with a bandwidth of 24.8 MHz (1%), which is slightly less than designed (30 MHz). At 5.0 GHz, the measured insertion loss is 1.01 dB (0.25 dB in simulation) with a bandwidth of 51.2 MHz (50 MHz in design). The higher insertion loss is believed to be due to the use of brass posts. The imperfect connections at the input and output coupling rods also contribute to higher loss. The first spurious passband

is observed at 6.9 GHz. The spurious passband can be moved to higher frequencies by using smaller cavities and higher capacitive loading, i.e. larger and/or higher posts.

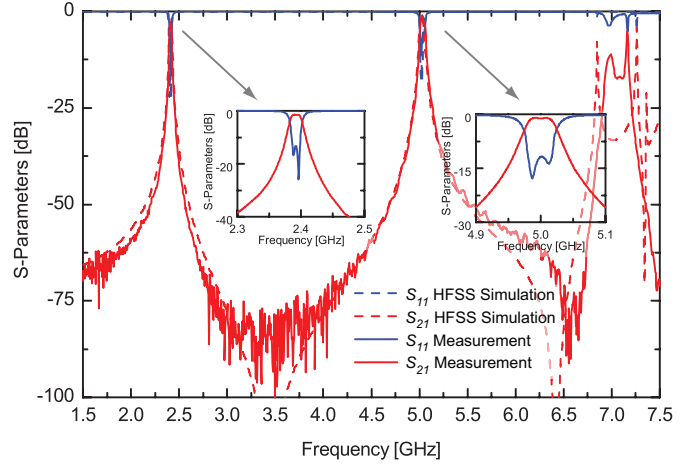


Fig. 7. Measurement results of the fabricated dual-band (2.4 GHz and 5.0 GHz) filter. The first spurious band is observed around 6.9 GHz.

V. CONCLUSION

We have presented a novel and flexible design approach for dual-band cavity filters. By changing the sizes and positions of the two capacitive loading posts in the DCL resonators, the center frequencies, as well as the inter-resonator and external coupling coefficients can be individually adjusted for different frequency and bandwidth requirements for the two passbands. An example 2-pole dual-band filter at 2.4 GHz and 5.0 GHz is fabricated to validate the proposed design approach.

REFERENCES

- [1] H. Miyake, S. Kitazawa, T. Ishizaki, T. Yamada, Y. Nagatomi, "A miniaturized monolithic dual band filter using ceramic lamination technique for dual mode portable telephones", *IEEE MTT-S International Microwave Symposium Digest*, vol.2, pp.789-792, June 1997
- [2] L.-C. Tsai, C.-W. Hsue, "Dual-band bandpass filters using equal-length coupled-serial-shunted lines and Z-transform technique", *IEEE Transactions on Microwave Theory and Techniques*, vol.52, no.4, pp. 1111-1117, April 2004
- [3] G. Macchiarella, S. Tamiazzo, "Design techniques for dual-passband filters", *IEEE Transactions on Microwave Theory and Techniques*, vol.53, no.11, pp. 3265-3271, Nov. 2005
- [4] X.-P. Chen, K. Wu, Z.-L. Li, "Dual-Band and Triple-Band Substrate Integrated Waveguide Filters With Chebyshev and Quasi-Elliptic Responses," *IEEE Transactions on Microwave Theory and Techniques*, vol.55, no.12, pp.2569-2578, Dec. 2007
- [5] J.-S. Hong, W. Tang, "Dual-band filter based on non-degenerate dual-mode slow-wave open-loop resonators", *IEEE MTT-S International Microwave Symposium Digest*, pp.861-864, 7-12 June 2009
- [6] C.-H. Lee; C.-I. G. Hsu, C.-C. Hsu, "Balanced Dual-Band BPF With Stub-Loaded SIRs for Common-Mode Suppression," *IEEE Microwave and Wireless Components Letters*, vol.20, no.2, pp.70-72, Feb. 2010
- [7] M. Jiang, L.-M. Chang, A. Chin, "Design of Dual-Passband Microstrip Bandpass Filters With Multi-Spurious Suppression," *IEEE Microwave and Wireless Components Letters*, vol.20, no.4, pp.199-201, April 2010
- [8] High Frequency Structure Simulator, Ansoft Cooperation. <http://www.ansoft.com/products/hf/hfss/>
- [9] G. Bianchi, R. Sorrentino, "Electronic filter simulation & design", McGraw-Hill Professional, 2007
- [10] D. Kajfez, E. J. Hwan, "Q-Factor Measurement with Network Analyzer," *IEEE Transactions on Microwave Theory and Techniques*, vol.32, no.7, pp. 666-670, Jul 1984